The Anisotropic Multifractal Model and Wind Turbine Wakes

G. Fitton[1], I. Tchiguirinskaia[1], D. Schertzer[1] & S. Lovejoy[2]
[1]Universitè Paris Est, Ecole des Ponts ParisTech, LEESU,
6-8 avenue B. Pascal, Citè Descartes, 77455, Marne-la-Vallée cedex 02, France;
tel.: +33 1 64 15 36 07, fax: +33 1 64 15 37 64
McGill University, Physics department, 3600 University street, Montreal, Quebec, Canada
E-mail: fittong@cereve.enpc.fr

Keywords: Universal Multifractals, Spectral Analysis, Wind Velocity Fluctuations and Power Estimation.

1 Introduction

A typical routine in wind field resource assessment, at the most basic level, consists of first to third order statistics of times series data. The quality of the time series data can range between 0.05 to 600 seconds. More often than not the frequency of data will be the latter of the two since it is the cumulative power over long periods of time that define the financial return from turbines and thus high-resolution data is deemed unnecessary. It is now evident that such coarse time series data are no longer sufficient for a representative assessment of the wind and that estimations based on such data are associated with inaccurate power curve prediction and turbine damage. In particular it has been suggested that such problems are due to a lack of understanding of the somewhat intermittent nature of the wind velocity fields and the small-scale fluctuations thus associated. In order to address this there has been a significant increase in research involving coupled mesoscale-microscale models and stochastic downscaling methods. Our contribution is a demonstration that a good knowledge of small-scale variability is essential for a better understanding of the atmospheric boundary layer. We discuss the applicability of the stochastic anisotropic multifractal model to the complex conditions of wind farm potential and operational sites.

2 Data

Available to us is six-months of wind velocity and temperature measurements at the heights 22, 23 and 43m.

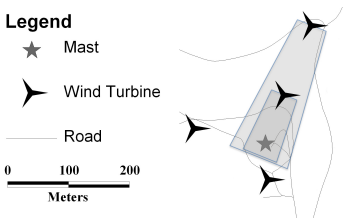

Figure 1: Schematic of turbine positions and wake effect due to North-Westerly winds (map courtesy of Julien Richard).

The measurements came from 3D sonic anemometers with a 10Hz data output rate positioned on a mast in a wind farm test site subject to wake turbulence effects (see Fig. 1). The quality of the data was of utmost importance so thorough pre-processing and verification was implemented to assure the reliability of the results.

3 Analysis

3.1 The Energy Spectrum and Scaling

A typical first-step-method to determine the overall scaling behaviour is the transformation of the velocity field into Fourier space. We 'should' then be able to observe power-law behaviour of the spectrum such that

$$E(\omega) \equiv A\omega^{-\beta} \tag{1}$$

where ω is the frequency, $E(\omega)$ is the energy at a given frequency, A is a coefficient of proportionality and β is the scaling exponent. The review of [Marusic et. al., 2010] discusses the existence of a -1 power law sub-range over small frequencies, adjoined by a classical Kolmogorov inertial sub-range with $\beta = 5/3$.
We will present shortly a more in-depth discussion on how our results compare to Kolmogorov's predictions however before this we would like to discuss the fact that there is no unique scaling regime i.e. there are three common scaling features, instead of the predicted universal law (see Figs. 2 and 3 also), that are:

- **High frequency scaling range** (R_{HF}:$\sim$ 0.1 secs to $\sim$5 mins) in which all three velocity components, u, v and w, follow (approximately) the same scaling law.
- **Mid-frequency w-component departure** from scaling at $\sim$5 minutes. Mid-Frequency, R_{MF}, corresponds to the ranges $\sim$ 5 mins to $\sim$1 hour.
- **Low frequency scaling reunification** (R_{LF}:$\sim$ 1 hr to $\sim$1 day) for all three velocity components at about an hour. The power law is not the same as that for small scales as will be discussed later.

The focus therefore of our more in-depth analysis is the behaviour of the horizontal u- and v-components over the mid-frequency-ranges i.e. $\sim$5 mins to $\sim$1 day. In fact what we

found was that our data fell into two categories; days (i.e., independent samples of 2^{19} measurements [$\approx$ 14.5 hours] per day) *without* a mid-frequency perturbation (Fig. 2) and days *with* a mid-frequency perturbation (Fig. 3). In the next section we will consider the simpler of the two regimes that are the non-perturbed days.

3.2 Non-perturbed Days & The Anisotropic Multifractal Model

The results from spectral analysis on non-perturbed days confirm a unique power law for all three velocity components over higher frequencies up to approximately 40 seconds at which the vertical wind w-component shows a clear scaling break followed by a -1 power law subrange as described in the previous section.

Moreover, such a clear separation of power law subranges allows us to obtain an estimate of the integral length scale for the vertical wind component as suggested in [Monin & Yaglom, 1975], which in turn leads to an estimate of the Reynolds number of about 60,000. Thus, from dimensional analysis one may obtain a minimum Reynolds number of about 14,000. These estimates confirm that the investigated wind field exhibits fully developed turbulence.

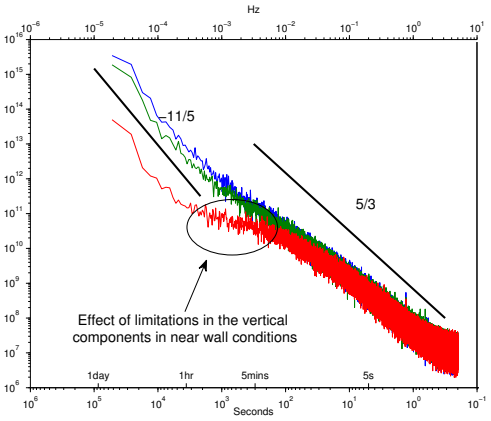

Figure 2: Averaged spectra for 11 non-perturbed days where the velocity component u is blue, v is green and w is red. The high-frequency range from ~ 0.1 sec to 5 mins has spectral slope ~ 1.4, less than the predicted 5/3. In addition we have highlighted the -1 adjoining range, from 5 mins to an hour, with the scale break being predictable based on the mast height (see [Fitton et. al., 2011] for more details). Low frequency scaling region is compatible with the -11/5 scaling law.

Over the high-frequency range Fig. 3 displays spectral exponents that differ from Kolmogorov's -5/3 law. The difference corresponds to an intermittency correction of spectral slopes and can be taken into account using the universal multifractal framework (Schertzer and Lovejoy, 1987), where:

- the energy density flux is a conserved (at any scale ratio λ) multifractal field proportional to a power law with singularity, γ, i.e.

$$\varepsilon_\lambda \propto \lambda^\gamma, \tag{2}$$

- the statistical moments of the energy density flux are defined by:

$$\langle \varepsilon_\lambda^q \rangle \propto \lambda^{K(q)}, \tag{3}$$

- and the scaling moment function $K(q)$ is defined by:

$$K(q) = \frac{C_1}{\alpha - 1}\left(q^\alpha - q\right). \tag{4}$$

Here, q, is the order of moment, C_1 is the codimension of the mean singularity and α is the multifractal Lévy index. The spectral exponent of Eq. 1 now becomes

$$\beta = 2H + 1 - K(2) \tag{5}$$

where $H = 1/3$ quantifies the degree of non-conservation of velocity increments. For spectra (i.e. for second order statistics), we estimated $K(2) = 0.27$. Such high intermittency corrections are expected over high frequencies in areas with high Reynolds numbers and complex terrain.

In addition we observed the Bolgiano-Obuhkov -11/5 power law at low frequencies illustrating the influence of large-scale vertical motions specific to the topography of our wind farm test site [Faggio & Jolin, 2003].

To take into account the dominant role of the vertical motion of large scale atmospheric structures, one may consider that the buoyancy force variance flux, ϕ, plays the same role as the energy flux, ε, in 3D turbulence but only along the vertical [Schertzer & Lovejoy, 1984]. This is contrary to the classical 'buoyancy subrange' that postulates an isotropic turbulence [Bolgiano, 1959, Obukhov, 1959] with two different (horizontal and vertical) scaling regimes. Thus we have the coupled sets of scaling equations [Schertzer & Lovejoy, 1984, Lazarev et. al., 1994]:

$$\left.\begin{aligned} \Delta V(\Delta x) &\stackrel{d}{=} (\varepsilon(\Delta x))^{1/3}\Delta x^{1/3} \\ \Delta V(\Delta z) &\stackrel{d}{=} (\phi(\Delta z))^{1/5}\Delta x^{3/5} \end{aligned}\right\} \tag{6}$$

$$\Longrightarrow (\varepsilon(\Delta x))^{1/3} \approx (\phi(\Delta z))^{1/5} \text{ when } \Delta x^{1/3} \approx \Delta z^{3/5} \tag{7}$$

where $\Delta V(\Delta x)$ and $\Delta V(\Delta z)$ denote the horizontal and vertical shears of the horizontal wind respectively and the symbol $\stackrel{d}{=}$ means equality in probability distribution.

Because the scaling fluctuations of both fluxes are not neglected (due to their explicit scale dependency) we can define anisotropic scaling (as defined by the anisotropic multifractal model [Schertzer & Lovejoy, 1984]) at all significant scales instead of two isotropic regimes, separated by a scaling break (see [Fitton et. al., 2011] for more details).

3.3 Perturbed Days, Wakes and Power Estimation

In [Fitton et. al., 2011] we put forward the argument that the non-perturbed days were a result of lack of influence of wind turbines justified by the low frequency power law (cross-diagonal mean wind) of the integrated cospectral analysis. The same argument allowed us to select days that were highly perturbed. By this we mean days where the mid-frequency range, R_{MF}, in which the scaling of horizontal

velocity components remained the same as described in the previous section, now have significant fluttering (see below [Fig. 3]).

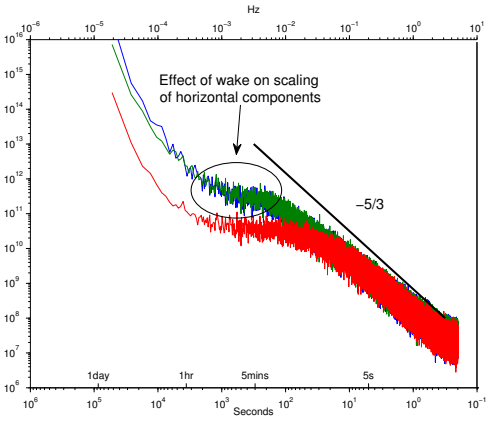

Figure 3: Averaged spectra for 11 perturbed days where the velocity component u is blue, v is green and w is red. The high-frequency range from ~ 0.1 sec to 5 mins has spectral slope ~ 1.6 which is much closer to the predicted 5/3. We have highlighted the fluttering for the horizontal components over R_{MF}. We can also see the fluttering of the vertical component is accentuated to a plateau. The 11/5 low frequency scaling regime remains, although with a lower coefficient of proportionality A (Eq. 1).

To see the effect of the turbines we can do a direct comparison of the integrated spectra, $\omega E(\omega)$, in log-linear coordinates of perturbed and non-perturbed days (11 of each see Fig. 4).

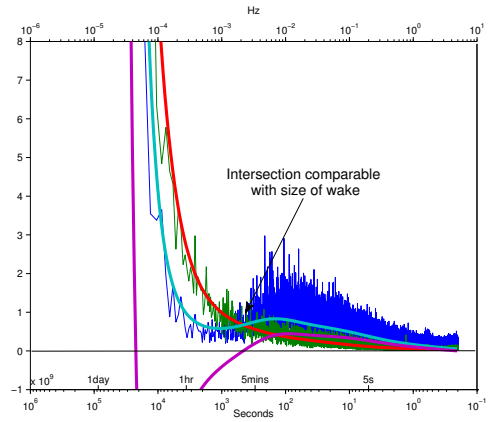

Figure 4: Comparison of perturbed and non-perturbed, u-component averaged integrated spectra, $\omega E(\omega)$, in log-linear coordinates; blue is perturbed days with light-blue moving average, green is non-perturbed with red moving average and purple is the differences of the moving averages.

This gives us a quantification of the energy per frequency increment making the overall evaluation of the energy gains and losses much easier. We have selected the horizontal u-component since there is no -1 adjoining range for non-perturbed days making it easier to make the comparison. Note the behaviour of the horizontal v-component is very similar (evidence of asymmetry at larger scales). From Fig. 4 we can draw the following intermediate conclusions based on the ranges defined in §3.1:

- **High frequency scaling range** (~ 0.1 secs to $\sim$5 mins) has an injection of energy since perturbed days (blue integrated spectra, light-blue moving average in Fig. 4) have more energy than the unperturbed days (green integrated spectra, red moving average in Fig. 4). This is confirmed by the positive difference of the moving average of the integrated spectra (purple curve of Fig. 4). If we consider the most basic approximation to a turbine, the actuator disc, then we can assume any eddy larger than the disc will be split into smaller eddies. This may explain the increase in high frequency energy. In fact, we can further confirm this idea since the transition of energy peaks at $\sim$ 5 mins highlighted again in Fig. 4 correspond to the size of the wake shown in Fig. 1.

- **Mid-frequency u-component** ($\sim$ 5 mins to $\sim$3 hours) shows evidence of energy pumping from the turbines for the perturbed days. This is more obvious when looking at the negative difference of the two integrated spectra over this range.

- **Low frequency** ($\sim$ 3 hours to $\sim$ 1 day [mesoscales]) shows that although there is similar scaling behaviour the energy for the perturbed days (red curve) is greater than the non-perturbed (light-blue curve) since the difference of the two (purple line) is positive. In [Fitton et. al., 2011] we suggested this was because the two particular types of wind the site was typically subject were strong North-Westerlys and weak South-Easterlys. This meant only the stronger winds would interact with the turbines (see Fig. 1).
  In addition we see at $\sim$ 3 hours the energy of the non-perturbed days becomes greater than perturbed. In the previous section we discussed how topographical features can change the scaling power law over the lower frequency data. This suggests there are similar topographical influences causing the loss of energy e.g. higher mean winds dissipate more energy over complex terrain.

Fig. 5 displays a schematic diagram that illustrates the corresponding inter-relations of different scaling ranges of the energy spectra. Over each of these ranges, two distinct power laws describe the corresponding scaling behaviour, with and without wake effects. Thus, from Eq. 5 we get:

$$E_1(\omega) = A_1 \omega^{-\beta_1}, \tag{8}$$

$$E_2(\omega) = A_2 \omega^{-\beta_2}. \tag{9}$$

Since the estimates of the multifractality parameter, α, remain stable for both perturbed and non-perturbed fields, the

ratio of the energy spectra is defined by the second order structure function:

$$\frac{E_1(\omega)}{E_2(\omega)} = \frac{A_1}{A_2}\omega^{-\zeta_\Delta(2)} \quad (10)$$

where $\zeta_\Delta = 2(\Delta H) - (\Delta C_1/(\alpha-1)) \cdot (2^\alpha - 2)$ from Eqs. 4 and 5.

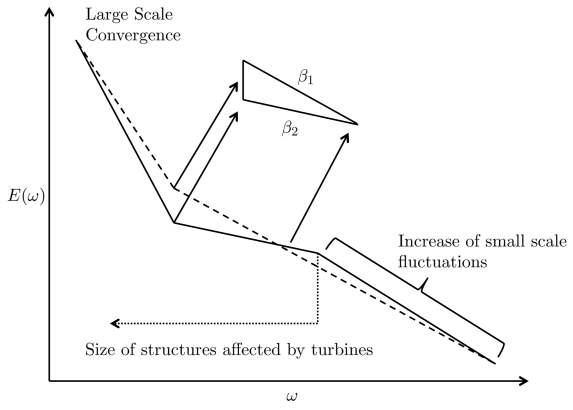

Figure 5: Schematic of the inter-relations of different scaling ranges of the energy spectra in a log-log plot.

From Fig. 5, Eq. 4 and the above equation (Eq. 10) we see an empirical spectral exponent closer to the theoretical values of $\beta = 5/3$ (over small scales) or $\beta = 11/5$ (over large scales), correspond to a smaller intermittency correction $K(2)$. Figs. 4 and 5 therefore suggest that by taking the energy over large scales, wind turbines create additional small-scale eddies and re-inject them as part of the energy over smaller scales, making the turbulence more homogeneous.

4 Conclusion

The aim of this study was to explore the scaling behaviour of atmospheric velocity measurements in a wind farm test site subject to wake turbulence effects. Based on this study we can make the following conclusions:

- Using long time series, 10Hz data, we identified (depending on the direction of the mean wind) two or three scaling sub-ranges.
- Through spectral analysis we found possible relations between wind velocity scaling breaks and associated theories of fully developed turbulence in the atmospheric surface-layer and used the universal multifractal framework to deal with the strong intermittency of the field.
- We have discussed how the anisotropic multifractal model can be applied to near wall atmospheric turbulence over complex terrain how it can be fully validated for days with no interaction with the wind turbine wakes.
- We found empirical evidence of the influence of wakes and suggested reasoning and scaling techniques that enable us to quantify the loss of energy with the potential of taking this into account using the anisotropic multifractal model.
- And finally, we discussed how the pumping of energy from wind turbines over mid-frequency scales, creates additional small-scale eddies which are re-injected as part of the energy over smaller scales. This makes the turbulence more homogeneous over the smaller scales in an analogous way to grid-generated homogeneous turbulence.

References

[Bolgiano, 1959] Bolgiano, R. 1959 Turbulent spectra in a stably stratified atmosphere, *J. Geophys. Res.* **64**, 2226.

[Faggio & Jolin, 2003] Faggio, G. & Jolin, C. 2003 Suivi ornithologique sur le parc dèoliennes dErsa- Rogliano (Haute Corse) - Rapport final-SIIF/AAPNRC-GOC, 100p.

[Fitton et. al., 2011] Fitton, G. F., Tchiguirinskaia, I., Schertzer D., & Lovejoy, S. 2011 Scaling Of Turbulence In The Atmospheric Surface-Layer: Which Anisotropy?, *Journal of Physics: Conference Series* (in review) Warsaw, ETC13.

[Lazarev et. al., 1994] Lazarev, A., Schertzer, D., Lovejoy, S. & Chigirinskaya, Y. 1994 Unified multifractal atmospheric dynamics tested in the tropics: part II, vertical scaling and generalized scale invariance, 115-123.

[Marusic et. al., 2010] Marusic, I., McKeon, B. J., Monkewitz, P. A., Nagib, H. M., Smits, A. J. & Sreenivasan, K. R. 2010 Wall-bounded turbulent flows at high Reynolds numbers: Recent advances and key issues *Phys. Fluid.*, **22**, 065103.

[Monin & Yaglom, 1975] Monin, A. S. & Yaglom, A. M. 1975 *Statistical Fluid Mechanics*, Cambridge, MIT-Press, Vol. 2, pp. 874.

[Obukhov, 1959] Obukhov, A. N. 1959 Effect of Archimedian forces on the structure of the temperature field in a temperature flow, *Sov. Phys. Dokl.* **125**, 1246.

[Pinus et. al., 1967] Pinus, N. Z., Reiter, E. R., Shur, G. N. & Vinnichenko, N. K. 1967 Power spectra of turbulence in the free atmosphere, *Tellus* **19**, 206.

[Schertzer & Lovejoy, 1984] Schertzer, D. & Lovejoy, S. 1984 On the Dimension of Atmospheric motions. In: T. Tatsumi (Editor), Turbulence and Chaotic phenomena in Fluids, Amsterdam, Elsevier Science Publishers B. V., pp. 505-512.

[Yaglom & Kader, 1989] Yaglom, A. M., Kader, B. A., & Zubkovskii, S. L. 1989 Spatial Correlation Functions of Surface-Layer Atmospheric Turbulence in Neutral Stratification, *Bound.-Lay. Meteorol.* **47**, pp. 233-249.